



**HAL**  
open science

## **Persistent neuromuscular disorders associated with changes in tibialis anterior and gastrocnemius lateralis muscle architecture in long-covid: an observational longitudinal study**

Isabella da Silva Almeida, Leandro Gomes de Jesus Ferreira, Gerson Cipriano, Rochelle Rocha Costa, Marco Aurélio Vaz, Nicolas Babault, Rita de Cássia Marqueti, João Luiz Quagliotti Durigan

### ► **To cite this version:**

Isabella da Silva Almeida, Leandro Gomes de Jesus Ferreira, Gerson Cipriano, Rochelle Rocha Costa, Marco Aurélio Vaz, et al.. Persistent neuromuscular disorders associated with changes in tibialis anterior and gastrocnemius lateralis muscle architecture in long-covid: an observational longitudinal study. *Scientific Reports*, 2025, 15 (1), pp.34375. <10.1038/s41598-025-17126-7>. <hal-05477175>

**HAL Id: hal-05477175**

**<https://hal.science/hal-05477175v1>**

Submitted on 26 Jan 2026

HAL is a multi-disciplinary open access archive for the deposit and dissemination of scientific research documents, whether they are published or not. The documents may come from teaching and research institutions in France or abroad, or from public or private research centers.

L'archive ouverte pluridisciplinaire HAL, est destinée au dépôt et à la diffusion de documents scientifiques de niveau recherche, publiés ou non, émanant des établissements d'enseignement et de recherche français ou étrangers, des laboratoires publics ou privés.



Distributed under a Creative Commons CC BY-NC 4.0 - Attribution - Non-commercial use - International License



## OPEN Persistent neuromuscular disorders associated with changes in tibialis anterior and gastrocnemius lateralis muscle architecture in long-covid: an observational longitudinal study

Isabella da Silva Almeida<sup>1,2</sup>✉, Leandro Gomes de Jesus Ferreira<sup>1,3</sup>, Gerson Cipriano Jr.<sup>1</sup>, Rochelle Rocha Costa<sup>2</sup>, Marco Aurélio Vaz<sup>4</sup>, Nicolas Babault<sup>5</sup>, Rita de Cássia Marqueti<sup>1,3</sup> & João Luiz Quagliotti Durigan<sup>1,3</sup>✉

Long COVID-19 causes complications, affecting quality of life and work capacity. However, its long-term impact on lower limb neuromuscular function remains unclear. To evaluate neuromuscular electrophysiological disorders (NEDs) and muscle architecture of the tibialis anterior (TA) and triceps surae (TS) in individuals with moderate or severe COVID-19 compared to control group over 12 months. Seventy participants were divided into moderate-COVID ( $n=22$ ), severe-COVID ( $n=18$ ), and control ( $n=30$ ) groups. COVID groups underwent four assessments over one year. NEDs in the TA and gastrocnemius lateralis (GL) were assessed via stimulus electrodiagnostic testing, while TA and TS muscle architecture was evaluated using ultrasound. Participants with severe-COVID exhibited significantly higher chronaxie ( $p < 0.001$ ) in the TA at the first assessment, NEDs were observed in 55.55%, 33.33%, and 16.66% of participants across the first three assessments. GL showed 5.55% prevalence of NEDs. Echogenicity increased in TA and GL muscles in the severe-COVID group ( $p < 0.001$ ). An association was found between TA chronaxie and echogenicity in the COVID groups during the short-term assessment ( $p < 0.001$ ). Severe COVID-19 is associated with higher prevalence of NEDs in the TA muscle and persistent echogenicity increases, suggesting polyneuromyopathy in the TA and widespread echogenicity abnormalities in long COVID patients.

**Keywords** Chronaxie, Echogenicity, Muscle architecture, Long COVID, rehabilitation, clinicians

Neurological disorders and musculoskeletal complications, including a reduction in peripheral nerve conduction and muscle mass loss, have become increasingly recognized as persistent manifestations of long COVID-19<sup>1–4</sup>. Although many patients fully recover after the acute phase of the infection, a significant proportion experience long COVID, which is characterized by symptoms that can persist for weeks or even months<sup>4</sup>. This new condition often presents debilitating symptoms, such as muscle fatigue and myalgia<sup>5–7</sup> substantially impacting quality of life and return-to-work activities, even 12 months after infection<sup>8</sup>. The mechanism by which the disease affects nerves is multifactorial and not yet well established<sup>9</sup>. However, it is hypothesized that the effects associated

<sup>1</sup>Laboratory of Muscle and Tendon Plasticity, Graduate Program in Rehabilitation Science, Faculdade de Ceilândia, Universidade de Brasília, Distrito Federal, Brazil. <sup>2</sup>Graduate Program in Physical Education, Physical Education Department, Universidade de Brasília, Distrito Federal, Brasília, Brazil. <sup>3</sup>Laboratory of Molecular Analysis, Graduate Program in Rehabilitation Science, Faculdade de Ceilândia, Universidade de Brasília, Distrito Federal, Brazil. <sup>4</sup>Exercise Research Laboratory, School of Physical Education, Physiotherapy and Dance, Federal University of Rio Grande do Sul, Porto Alegre, Brazil. <sup>5</sup>Centre d'Expertise de la Performance, Sports Science Faculty, INSERM U1093 CAPS, University of Burgundy, BP 27877, Dijon, Dijon 21078, France. ✉email: isabellafsioucb@gmail.com; durigan@unb.br

with muscle disuse, may lead to systemic alterations, such as polyneuropathy, contributing to neuromuscular electrophysiological disorders (NEDs)<sup>9–11</sup>.

NEDs have been identified in long COVID patients<sup>1,7</sup> with a higher prevalence observed among older individuals<sup>12</sup>. These disorders can be assessed using a non-invasive method called the stimulus electrodiagnostic test (SET), which employs specific parameters of neuromuscular electrical stimulation commonly used by physical therapists in clinical settings<sup>9,11,13</sup>. The SET evaluates nerve and muscle responses by measuring chronaxie, the shortest pulse duration needed to reach neuromuscular excitability at a current intensity twice the rheobase value, which refers to the minimal current intensity needed to elicit a muscle response<sup>9,14,15</sup>. Additionally, the accommodation index (AI), another key parameter, is the ratio between the threshold amperage of a slowly rising impulse and the threshold amperage of a suddenly rising rectangular impulse<sup>9,14</sup>. Chronaxie values of  $\geq 1$  ms are indicative of a NED<sup>14,15</sup>, highlighting the SET as a valuable tool for screening and for the initial assessment in suspected cases of NEDs<sup>9,14,15</sup>.

Hospitalization and prolonged bed rest can lead to polyneuropathy, affecting the peripheral nervous system and muscle structure, and resulting in muscle weakness and functional impairments<sup>11,16–18</sup>. In mechanically ventilated patients, the tibialis anterior (TA) muscle showed a significant prevalence of NED<sup>11</sup>. Although the mechanisms underlying long COVID remain unclear, changes in muscle architecture can contribute to persistent musculoskeletal symptoms<sup>19,20</sup>. Muscle architecture, referring to the arrangement of muscle fibers with respect to the muscle tendons, directly influences the axis of force generation and overall muscle function, and can be reliably assessed using B-mode ultrasonography<sup>13,21,22</sup>. COVID-19 patients exhibited reduced cross-sectional area (CSA) and muscle thickness (MT) in the quadriceps muscles, along with increased echogenicity, indicating diminished muscle quality within the first 10 days of hospitalization<sup>19</sup>. Similarly, even 6 months after infection, Appelman et al. (2024) reported a reduction in the CSA of type 1 fibers of the vastus lateralis muscle in individuals with long COVID<sup>20</sup>. It is important to highlight that, although previous studies have investigated the neuromuscular<sup>1,7</sup> or muscular consequences<sup>19,20</sup> of long COVID in isolation, there is still a lack of trials that have simultaneously assessed, in a one-year longitudinal approach, the prevalence of NEDs and muscle architecture in comparison with healthy individuals. This integrated approach is essential for a deeper understanding of the infection's impact on neuromuscular and structural function over time.

Understanding both the neurological disorders and musculoskeletal complications associated with COVID-19 in an integrated manner is essential for assessing its impact on electrical neuromuscular function and muscle architecture. Studying these factors together provides critical insights that can significantly enhance rehabilitation strategies for patients suffering from long-term effects of COVID-19. Therefore, the current study aimed to investigate the neuromuscular function and muscle architecture of the TA and triceps surae (TS) muscles in participants with moderate or severe COVID-19, compared to a control group, over a one-year post-infection period. Our hypothesis was that the severity and timing of disease assessment would affect the musculoskeletal and neural systems, negatively impacting peripheral nerve conduction and muscle architecture, and leading to increases in chronaxie and muscle echogenicity.

## Materials and methods

### Study design

This Level 2 longitudinal study was approved by the Institutional Review Board of the University of Brasília (CAAE 45043821.0.0000.8093) and conducted under the ethical standards of the Declaration of Helsinki. All participants provided informed consent prior to inclusion. Evaluations were conducted from September 2021 to October 2023. The manuscript is part of a larger observational study, with the full protocol available at ClinicalTrials.gov (NCT04961255) and reported according to the STROBE guidelines<sup>23</sup>.

### Participants

Participants were recruited through local clinics and hospitals via advertisement flyers. The inclusion criteria required participants to be aged between 18 and 80 years and to have a history of SARS-CoV-2 infection, classified as either moderate (moderate-COVID) or severe (severe-COVID). For moderate-COVID, a positive COVID-19 diagnosis was needed, verified through a molecular test (RT-PCR), a serological test to detect antibody reactivity, or an immunochromatographic test for antibodies and antigens. The individuals also needed to have experienced COVID-19 symptoms, such as dry cough, runny nose, sore throat, diffuse body pain, or persistent hyperthermia, without the need for hospital admission or evidence of hypoxemia. For severe-COVID, a positive test and hypoxemia ( $\text{SpO}_2 \leq 93\%$ ), requiring hospitalization were needed. The control group included individuals without a COVID-19 history or symptoms. Exclusion criteria included neuromuscular or orthopedic issues, pregnancy, active infections, or neurological conditions that could interfere with data collection<sup>24,25</sup>.

### Procedures

All participants followed a standardized protocol, with four laboratory visits over 12 months, except the control group, which was assessed only once to ensure they would not be infected with SARS-CoV-2 throughout the study follow-up. The first assessment (A21-30) occurred between the 21st and 30th days after symptom onset for moderate-COVID and after hospital discharge for severe-COVID, followed by the second assessment (A31-90) which took place between the 31st and 90th days, the third (A91-180) between the 91st and 180th days, and the fourth (A181-360) between the 181st and 360th days after symptom onset (moderate-COVID) and after hospital discharge (severe-COVID). All evaluations were conducted by the same assessors (ISA and LGJF) at the same time of day. Before the assessments, participants were informed and familiarized with the procedures. Demographic and clinical information were collected, and perception of fatigue was assessed using the Fatigue Severity Scale questionnaire<sup>26</sup> during each assessment. First, the SET was performed, followed by muscle architecture analysis. Skin was cleaned with 70% alcohol swabs to minimize impedance.

### Electrical neuromuscular abnormality assessment

The SET was performed to evaluate NEDs in the TA and gastrocnemius lateralis (GL) muscles. The GL muscle was chosen to represent the TS muscle due to its accessibility for examination and the high reliability demonstrated in previous assessments, both in SET<sup>9</sup> and in ultrasound measurements<sup>21</sup>. The test was conducted after identifying the motor points of the two target muscles<sup>27</sup>. A universal pulse generator (Dualpex 071, Quark Medical LTDA) was used with a reference electrode (anode; 100 cm<sup>2</sup>) placed on the patella. An active pen electrode (cathode; 1 cm<sup>2</sup>) was used to locate the motor points and perform the test<sup>9,27</sup>. The rheobase was measured using a monopolar current with a rectangular pulse with a 1-second duration, 2-second rest interval, and frequency of 1 Hz, and gradually increasing the current intensity until a slight muscle contraction was visible<sup>9,28</sup>. For the chronaxie, a current intensity that was double that of the rheobase was employed, with adjustments made to the pulse duration (following the available device values) from 20  $\mu$ s to 1 s, until a visible contraction was observed<sup>9,22,28</sup>. For accommodation, a monopolar current with an exponential pulse was utilized, featuring a pulse duration of 1 s and a 2-second interval. The current was increased from 0 to 69 mA in 1 mA increments until a visible muscle contraction occurred<sup>9,14,22,29</sup>. The AI was calculated by dividing the accommodation by the rheobase<sup>9,14,22</sup>. The reliability of these methods has been well-established and is considered good to excellent<sup>9</sup>.

### Muscle ultrasound imaging

The pennation angle (PA), fascicle length (FL), MT, and echogenicity were assessed using a B-mode ultrasound system (M-Turbo, Sonosite, Bothell, WA, USA), equipped with a 7.5 MHz linear transducer and set to a depth of 6 cm, with a frame rate of 30 Hz. Three images were obtained for each participant, and the average values of the outcomes were used. For the TA imaging, participants were positioned in supine with a slight knee bend to relax the muscles and minimize fascicle curvature<sup>21,30</sup>. Imaging of the soleus (SO), GL, and gastrocnemius medialis (GM) muscles was performed with participants in a prone position, legs fully extended, and ankles maintained in a neutral position without any change in joint angle during the examination<sup>21,31</sup>. For PA, FL, and MT measurements, the probe was positioned longitudinally along the muscle, while for echogenicity the probe was placed transversely to the muscle belly. The TA architecture was measured at the proximal quarter of the distance between the lower border of the patella and the lateral malleolus, with the probe positioned on the anterolateral aspect of the leg<sup>21,32</sup>. The GL, GM, and SO were assessed at 30%, 30%, and 50% of the distance from the popliteal crease to the lateral malleolus, respectively<sup>21,33,34</sup>. A transparent plastic sheet was used to map anatomical landmarks and the exact probe placement site during the initial assessment. This map was realigned with the participant's skin at each follow-up to ensure consistent probe positioning across all time points and muscles, minimizing variability and enhancing measurement reliability, as adapted from a previous study<sup>35</sup>. PA was defined as the angulation of muscle fibers relative to the muscle's line of force, determined by measuring the angle between the muscle fibers and the deep aponeurosis<sup>21,36</sup>. FL was defined as the total length of the muscle fiber<sup>21,30</sup>. MT was assessed by marking five vertical lines along the ultrasound image, each representing the thickest area between the superficial and deep aponeurosis<sup>21,32</sup>. To evaluate muscle echogenicity, a region of interest was defined using a tracing technique, ensuring the inclusion of all visible muscle areas while excluding surrounding fascia or bone<sup>21,37</sup>. Echogenicity was analyzed through a histogram on a grayscale scale ranging from 0 (black) to 255 (white)<sup>18,21,38</sup>, with the mean echogenicity calculated by averaging values from the three images for each muscle. The analyses were conducted using ImageJ software (National Institute of Health, Bethesda, MD, USA). Good to excellent reliability has been established in these methods<sup>21</sup>.

### Statistical analysis

The Generalized Estimating Equations (GEE) method with gamma distribution, logarithmic link function, robust estimator covariance matrix and independent working correlation matrix structure was used to assess differences both between and within groups, using “group” and “assessments” as factors across all outcomes. To determine the optimal functional correlation structure in the GEE analyses, the independence model criterion was applied<sup>39</sup>. The least significant difference procedure was used as a post hoc test to locate differences. The GEE method with gamma distribution, logarithmic link function, robust estimator covariance matrix and independent working correlation matrix structure was also employed to analyze sample characterization data, using “group” as a factor to compare means across the three groups for continuous variables. This method was also used to examine the interactions between “group” and “assessment”, in order to detect time-related differences in variables such as physical activity at the time of assessment and fatigue perception, measured by the Fatigue Severity Scale<sup>26</sup>. Categorical variables were compared using the Chi-Square Test. Thereafter, Spearman's correlation was performed to measure the relationship between chronaxie and muscle architecture variables, such as PA, FL, MT, and echogenicity. Multivariate analyses (using multiple linear regressions) were conducted to examine the association between chronaxie and the variables that showed a significant correlation (description of the analysis is presented in supplementary material 1) - echogenicity and MT - in the COVID groups across all assessments. Chronaxie association was analyzed only for the TA muscle due to the low NED prevalence in the GL. Due to the global impact of the COVID-19 pandemic, calculating the ideal sample size was not feasible because of the lack of prior data. However, post hoc power analyses were performed and can be found in Supplementary Table 3. The level of statistical significance adopted was  $\alpha=0.05$  and the statistical software SPSS version 22.0 (IBM Corporation, Armonk, NY, USA) was used.

### Results

The current study included 22 moderate-COVID participants, 18 severe-COVID patients, and 30 healthy controls, with 190 assessments conducted. Table 1 presents the participant characteristics.

	Groups			Pvalue
	Control group	Moderate-COVID	Severe-COVID	
	(n = 30)	(n = 22)	(n = 18)	
Characteristics	Mean (CI 95%)	Mean (CI 95%)	Mean (CI 95%)	
Sex (number of participants/% of participants)				
Male	13/43.33	10/45.45	8/44.44	0.988
Female	17/56.66	12/54.54	10/55.55	
Age (years)	46.53 (42.10–51.43)	38.27 (33.96–43.13) *	50.83 (45.19–57.18) #	0.001
Weight (kg)				
A21-30	69.54 (65.07–74.31)	71.28 (64.14–79.21)	83.08 (75.91–90.92) # *	0.001
A31-90		71.57 (64.50–79.42)	84.89 (77.27–93.25) a # *	
A91-180		72.32 (65.14–80.28)	85.43 (77.51–94.15) a # *	
A181-360		73.12 (65.96–81.08) a, c	87.49 (79.89–95.81) a, b, c # *	
Height (m)	1.66 (1.63–1.69)	1.66 (1.62–1.70)	1.61 (1.55–1.66)	0.206
BMI (kg/m <sup>2</sup> )	24.91 (23.85–26.02)	25.55 (23.51–27.77)	31.94 (29.70–34.35) # *	0.001
Comorbidities (% of participants)				
Hypertension	16.66	4.54	66.66 #	0.001
Diabetes	0	4.54	38.88*	0.001
Dyslipidemia	20.00	13.63	50.00 #	0.021
Depression	0	4.54	27.77*	0.003
Anxiety	3.33	22.72	16.66	0.102
Panic Syndrome	0	4.54	11.11	0.183
Asthma	0	18.18	11.11	0.062
Hospitalization period (days)	NA	NA	38.38 (27.15–49.62)	NA
Period in ICU (days)	NA	NA	21.44 (13.72–29.16)	NA
COVID vaccine before infection (n) for moderate and severe-COVID groups and COVID vaccine at the time of assessment for the Control (% of participants)				
Yes	93.33	100	88.88	0.298
No	6.66	0	11.11	
Number of doses	3.50 (3.25–3.77)	2.14 (1.89–2.41) *	2.00 (1.72–2.32) *	0.001
Current smoking (% of participants)				
Yes	3.33	4.54	0	0.677
No	96.66	95.45	100	
Time (Years)	0.03 (0.00–0.06)	0.02 (0.00–0.05)	0.00 (0.00–0.00)	
Previous smoking (% of participants)				
Yes	16.66	31.81	33.33	0.323
No	83.33	68.18	66.66	
Time (years)	16.60 (8.40–32.79)	15.85 (11.00–22.85)	27.16 (19.67–37.51)	0.076
Interruption time (years)	24.40 (19.34–30.78)	10.37 (5.45–19.72) *	11.63 (5.77–23.42) *	0.011
Practice of physical activity before infection and at the time of assessment for the Control group (% of participants)				
Yes	63.33	40.90	27.77*	0.045
No	36.66	59.09	72.22	
Practice of physical activity at the time of assessment (% of participants)				
A21-30				0.001
Yes	63.33	36.36	16.66 #*	
No	36.66	63.63	83.33	
A31-90				
Yes		63.63	27.77 #*	
No		36.36	72.22	
A91-180				
Yes		77.27	27.77 #*	
No		22.72	72.22	
A181-360				
Yes		63.63	22.22**	
No		36.36	77.77	
Physiotherapy after infection (% of participants)				
Continued				

	Groups			
	Control group	Moderate-COVID	Severe-COVID	
	(n = 30)	(n = 22)	(n = 18)	
Yes	NA	0	72.22 *	0.001
No	NA	100	27.77	
Perception of fatigue (fatigue severity scale)				
A21-30	2.75 (2.33–3.24)	4.60 (4.09–5.16)*	5.52 (4.93–6.18)*#	0.001
A31-90		3.68 (3.08–4.40)*a	4.47 (3.85–5.20)*a	
A91-180		3.77 (3.24–4.38)*a	4.47 (3.87–5.17)*a	
A181-360		3.59 (3.01–4.29)*a	4.78 (4.03–5.67)*#	

NA, not applicable; \* = Different from the Control in the respective assessment; # = Different from moderate-COVID in the respective assessment; a = Different from A21-30; b = Different from assessment 2; c = Different from assessment 3. ( $p < 0.05$ ).

**Table 1.** Characteristics of the participants.

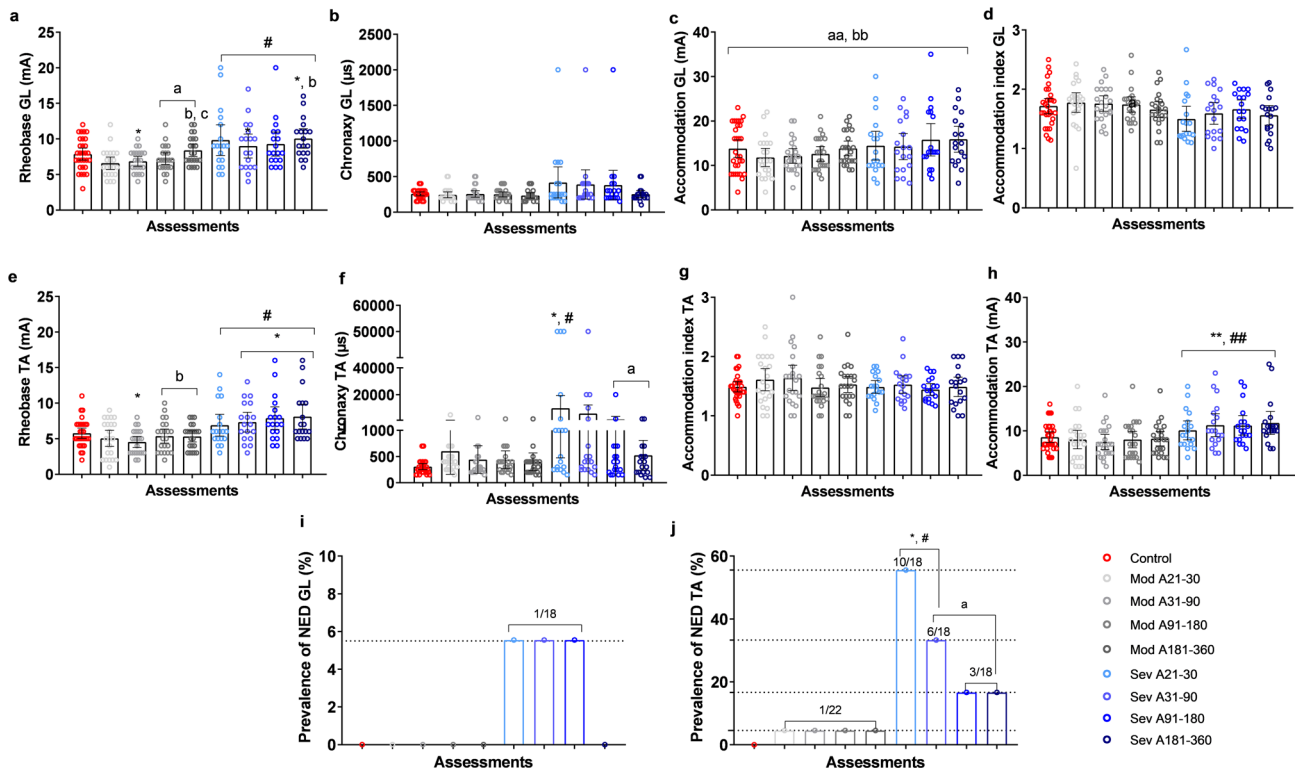


**Fig. 1.** Electrical neuromuscular abnormality assessment. a = different from A21-30 intragroup; b = different from A31-90 intragroup; # = different from moderate-COVID at the same assessment; \* = different from the Control; aa = different from A21-30, main effect of assessment; bb = different from A31-90, main effect of assessment; ## = different from moderate-COVID, main effect of group; \*\* = different from the Control, main effect of group. ( $p < 0.05$ ).

### Electrical neuromuscular abnormalities assessment

The SET results are presented in Fig. 1. All datasets related to the outcomes rheobase, accommodation, and AI are included in Supplementary Table 1.

For the chronaxie analysis, the GL assessment revealed no significant differences. For the TA chronaxie, a group-assessment interaction ( $p < 0.001$ ) demonstrated that the severe-COVID group had higher chronaxie values than both the moderate-COVID and control groups at A21-30 ( $p = 0.032$  and  $p = 0.027$ , respectively). In the intragroup comparisons, the severe-COVID group had lower chronaxie values at A91-180 ( $p = 0.029$ ) and A181-360 ( $p = 0.029$ ) compared to the A21-30 assessment.

### Prevalence of NEDs

The NED prevalence analysis for the TA muscle showed 4.54% in moderate-COVID across assessments A21-30, A31-90, and A91-180. In severe-COVID, the NED prevalence was 55.55% at A21-30, 33.33% at A31-90,

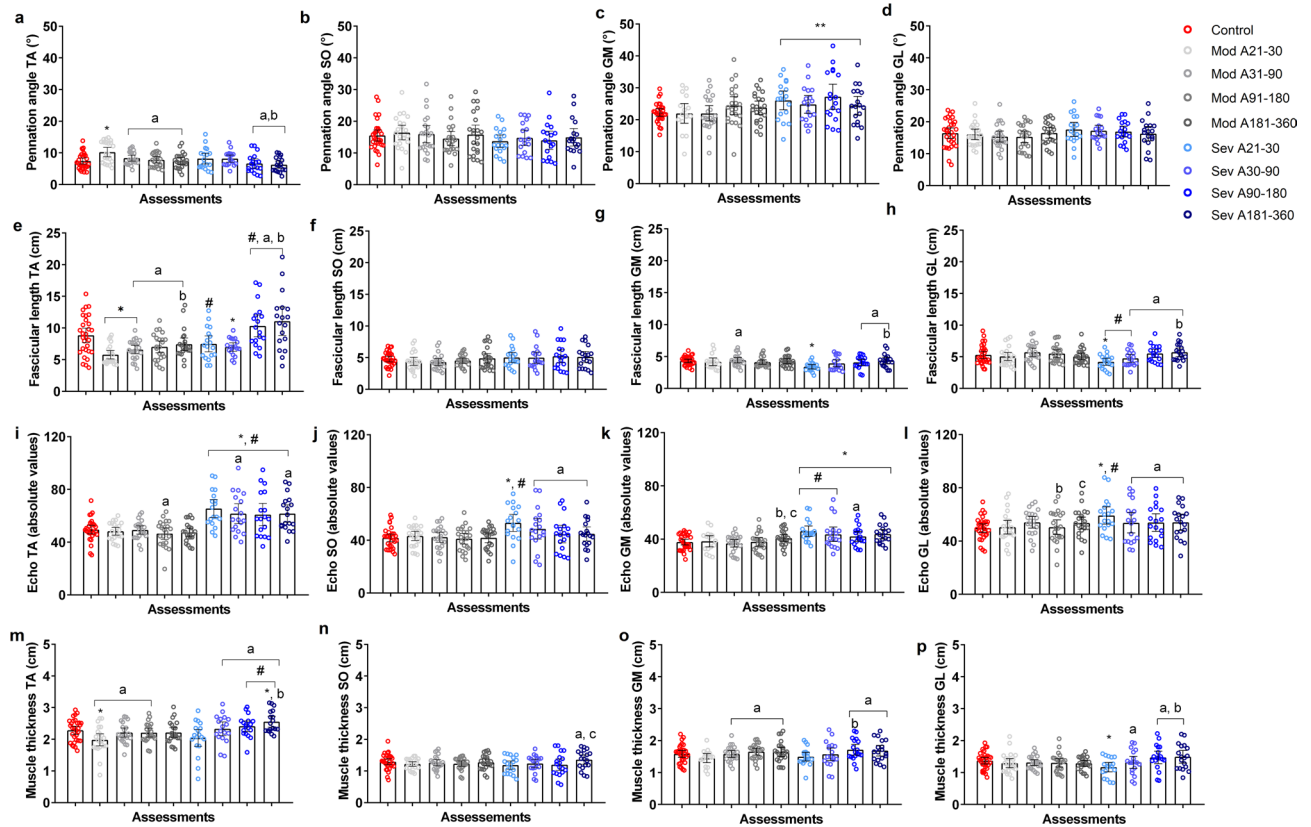


**Fig. 2.** Muscle ultrasound assessment. a = different from A21-30 intragroup; b = different from A31-90 intragroup; # = different from moderate-COVID at the same assessment; \* = different from the Control; \*\* = different from the Control, main effect of group. ( $p < 0.05$ ).

and 16.66% at A91-180 and A181-360. Severe-COVID exhibited significantly higher NED prevalence values compared to both the control and moderate-COVID groups at A21-30 ( $p < 0.001$ ) and A31-90 ( $p = 0.003$  and  $p = 0.016$ , respectively). In the intragroup comparisons, severe-COVID showed a significant decrease in NED prevalence in all assessments ( $p < 0.05$ ) compared to A21-30.

### Muscle ultrasound assessment

The results of the muscle ultrasound assessment are presented in Fig. 2. All datasets related to the outcomes PA, FL, and MT for the analyzed muscles are included in Supplementary Table 2.

Regarding the echogenicity analysis, for the TA muscle, a group-assessment interaction ( $p = 0.015$ ) revealed that severe-COVID presented higher values when compared with both moderate-COVID and control groups in all assessments ( $p < 0.05$ ). In the intragroup comparisons, severe-COVID presented lower values at A31-90 ( $p = 0.006$ ) and A181-360 ( $p = 0.02$ ) compared to A21-30, and moderate-COVID presented lower echogenicity at A21-30 ( $p = 0.047$ ) than the A91-180 assessment.

For the SO muscle, a group-assessment interaction ( $p < 0.001$ ) revealed that severe-COVID presented higher echogenicity compared to both the moderate-COVID ( $p = 0.004$ ) and control ( $p = 0.001$ ) groups at A21-30. In the intragroup comparisons, a decrease in echogenicity was observed in all assessments when compared to A21-30 ( $p < 0.05$ ) in severe-COVID.

In the GM analysis, the echogenicity evaluation revealed a group-assessment interaction ( $p < 0.001$ ), showing that severe-COVID had higher echogenicity than the control group across all assessments ( $p < 0.05$ ), and higher than moderate-COVID at A21-30 ( $p = 0.003$ ) and A31-90 ( $p = 0.017$ ). In the intragroup analysis, severe-COVID presented lower echogenicity at A91-180 compared to A21-30 ( $p = 0.001$ ), and moderate-COVID also showed higher echogenicity at A181-360 compared to A31-90 ( $p = 0.001$ ) and A91-180 ( $p = 0.034$ ).

For GL, a group-assessment interaction for echogenicity ( $p = 0.005$ ) revealed higher values in severe-COVID compared to both moderate-COVID ( $p = 0.022$ ) and control ( $p = 0.005$ ) groups at A21-30. In the intragroup analysis, severe-COVID showed higher echogenicity at A21-30 compared to all other assessments ( $p < 0.05$ ), and moderate-COVID also showed lower echogenicity at A91-180 compared to A31-90 ( $p = 0.03$ ) and A181-360 ( $p = 0.024$ ).

### Association with chronaxie

Multiple linear regression revealed a significant degree of prediction for chronaxie at assessments A21-30 ( $p < 0.001$ ), A31-90 ( $p < 0.001$ ), and A91-180 ( $p = 0.04$ ). For assessment A181-360, no significant prediction was

found ( $p=0.19$ ). Only echogenicity was considered a predictor for chronaxie at assessments A21-30 ( $p<0.001$ ), A31-90 ( $p<0.001$ ), and A91-181 ( $p=0.013$ ). In other words, for each unit increase in echogenicity, chronaxie increased by 652  $\mu$ s at assessment A21-30, by 467.61  $\mu$ s at assessment A31-90, and by 80.72  $\mu$ s at assessment A91-180 (more information is described in supplementary material 1).

## Discussion

According to our hypothesis, individuals who experienced severe COVID exhibited significantly higher chronaxie values and a higher prevalence of NEDs in the TA muscle, which was related to the timing of the assessment. The severe-COVID group also showed significant alterations in muscle echogenicity across all analyzed muscles, with a particular emphasis on the TA muscle. This aligns with the observed association between chronaxie and echogenicity in the TA muscle for the COVID groups. From a clinical perspective, these findings have important implications for planning rehabilitation strategies in patients with long COVID. Given the crucial roles of the TA and TS muscles in locomotion and daily activities<sup>40,41</sup> dysfunctions in these muscles could impact mobility and quality of life. Our results suggest that the TA muscle shows more pronounced changes than the TS, indicating that some muscles may be more susceptible to the impact of infection and disuse and highlighting the importance of assessing diverse muscles in terms of NEDs and muscle architecture. Clinicians should consider the time elapsed since the first COVID infection and a muscle-targeted approach as factors that can influence the benefits of optimizing rehabilitation, particularly in severe COVID patients. Tailoring rehabilitation strategies to focus on the specific muscles affected by the disease and adjusting the timing of interventions may optimize functional outcomes and improve patients' mobility and quality of life.

The mechanism of long COVID is not yet fully established. However, individuals who experienced a more severe form of the disease appear to have a worse prognosis<sup>8,42,43</sup>, with prevalent muscle symptoms, such as myalgia and fatigue<sup>5-7</sup>. In our study, participants in the severe COVID-19 group exhibited higher BMI, a greater number of comorbidities, advanced age, and lower levels of physical activity. These well-established risk factors not only increase the likelihood of developing more severe forms of COVID-19 and subsequent hospitalization but may also explain our findings<sup>44</sup>, as they predispose individuals to a poorer baseline health status<sup>44-46</sup>. The effects of prolonged hospitalization and bed rest, commonly experienced by patients with severe COVID-19, may contribute to neuromuscular dysfunction through mechanisms related to disuse<sup>19</sup>. Approximately 36.4% of patients hospitalized for COVID-19 exhibit neurological complications involving the peripheral nervous system, central nervous system, and skeletal muscles<sup>47</sup>. Muscle disuse is known to induce atrophy, reduce motor unit recruitment, alter neuromuscular excitability, and impair mitochondrial function, all of which can exacerbate functional impairments and hinder recovery<sup>18,48</sup>. Additionally, the pathophysiology of COVID-19 in the peripheral nervous system is linked to immune dysregulation and hyperinflammation, with nerve entrapment potentially occurring secondary to fluid accumulation and positioning for ventilation-perfusion optimization<sup>49,50</sup>. These disuse-related alterations may overlap with or potentiate the direct effects of SARS-CoV-2 on the neuromuscular system, complicating the clinical presentation and highlighting the need for comprehensive assessments.

In the current study, we used the SET, a physical therapy methodology that assesses evoked excitability through transcutaneous electrical stimulation of muscle and nerve tissue<sup>9,14,15</sup>. The SET was chosen for its affordability, non-invasiveness, and suitability in various clinical settings as an initial assessment for detecting NED<sup>9,11,22,28,51</sup>. It also demonstrated good inter- and intra-rater reliability in evaluating COVID-19 survivors<sup>9</sup>. Our results showed significantly elevated chronaxie values and a substantially higher prevalence of NEDs in the TA muscle among participants who had severe COVID-19, particularly during the first two assessments compared to the control and moderate COVID-19 groups. In the short-term assessment, 55.55% of severe-COVID participants presented NEDs, compared to 4.54% in the moderate-COVID group. While the NED prevalence remained low and stable in the control and moderate-COVID groups, it decreased but remained substantial in severe-COVID: 33.33% at the A31-90 assessment and 16.66% at the final two assessments. The higher prevalence of NED in the TA muscle among individuals who experienced severe COVID-19 is a critical finding, as this neuropathy has been reported among COVID-19 survivors<sup>52-56</sup>. The TA muscle is innervated by the peroneal nerve, and peroneal neuropathy generally presents as foot drop, or failure in dorsiflexion of the ankle and toes<sup>40,41</sup>. Our data suggests that individuals with varying levels of severity of an infection that causes both systemic effects and a significant decrease in activity may experience a direct impact on the neuromuscular junction or muscle fibers<sup>50</sup>. Additionally, the prone position, commonly used in COVID-19 patients with acute respiratory syndrome to optimize thoracic mechanics, is known to cause peripheral nervous system damage<sup>49,53</sup>. This highlights the need for a targeted approach to evaluate and detect NED, as these dysfunctions can significantly impact daily activities, increasing the risk of falls and injuries<sup>40,41</sup> and potentially influencing the design of rehabilitation programs for long COVID-19 patients.

In addition to NEDs, individuals with COVID-19 exhibit muscle weakness and sarcopenia<sup>57</sup>. While the causal link between COVID-19 and the muscle atrophy and weakness observed in survivors is unclear, these symptoms are prevalent in this population<sup>57</sup> and resemble the weakness associated with ICU-acquired conditions<sup>19,57</sup>. An important aspect to consider is the variability in hospitalization duration among participants in the severe group. Although all met the clinical criteria for severe COVID-19, the length of stay varied and may have influenced the neuromuscular and musculoskeletal outcomes observed. However, patients with severe and critical COVID-19 appear to experience a reduction in the CSA of the rectus femoris muscle and a decrease in the MT of the anterior compartment of the quadriceps, along with increased echogenicity, especially during the first to tenth day of hospitalization<sup>19</sup>. This suggests that even patients with shorter hospital stays may have experienced significant alterations<sup>19</sup>. Here, we observed localized changes in the TA muscle, including a reduction in PA and an increase in FL and MT across the assessments for the COVID groups. The severe-COVID group also showed increases in FL and MT in the GL and GM muscles. Our results can be explained by the reorganization of muscle fibers

during periods of disuse and immobilization, resulting from reduced mechanical stimulation<sup>31,58</sup>. This leads to a decrease in muscle CSA, often accompanied by a reduction in PA and FL<sup>31,58</sup>. These changes negatively impact force production and contraction speed, as these factors are linked to the number of sarcomeres arranged in series and parallel<sup>31,58</sup>. Participants with severe COVID may have experienced muscle architecture disorganization during the illness, which was reflected in the changes observed throughout the follow-up period. Finally, an increase in echogenicity was observed in all assessed muscles, particularly in the short-term assessment, further emphasizing the impact and changes caused by the disease during the acute phase.

The TA muscle demonstrated higher echogenicity across all assessments, suggesting a slower recovery process. Similarly, the TS also exhibited increased echogenicity compared to the control group, particularly in the GM muscle, showcasing its susceptibility to disuse. Antigravity muscles, such as the gastrocnemius, are more vulnerable to atrophy during prolonged immobilization, often showing a more pronounced reduction in thickness compared to muscles like the TA<sup>31</sup>. An increase in echogenicity may also indicate deterioration in muscle quality, likely due to infiltration of adipose and connective tissue, as well as muscle necrosis associated with muscle fiber remodeling<sup>19</sup>. Through multiple regressions, we found that echogenicity predicted chronaxie. Specifically, each unit increase in echogenicity can increase chronaxie by 652 to 80.72  $\mu$ s, suggesting, particularly for the TA muscle, a pattern where alterations in muscle architecture are linked to changes in neuromuscular function. This relationship may indicate that structural modifications in muscle fibers affect their functional capacity, potentially impairing overall muscle performance. Indeed, patients with long COVID who exhibit reduced exercise capacity appear to show metabolic alterations in skeletal muscle, associated with changes in muscle fiber profile and the presence of signs of muscle tissue damage<sup>20</sup>. Our findings align with previous studies that showed increased muscle echogenicity and elevated chronaxie values in hospitalized patients who developed NED<sup>11,59</sup>. Electromyographic abnormalities and neuromuscular histological changes have also been reported, suggesting the coexistence of motor axonopathies and myopathies in critically ill patients<sup>60</sup>. Altogether, our findings suggest that changes in echogenicity and chronaxie may be linked to the NED prevalence in patients who experienced more severe forms of COVID-19 and required hospitalization during the acute phase, reflecting the structural and functional impact of muscular alterations in these cases.

### Study limitations

Some limitations of this study should be acknowledged. First, it was not possible to perform a sample size calculation due to the lack of previous data in the literature. Given the constraints of the COVID-19 pandemic, a convenience sample was necessary to ensure participation. However, the significance of our findings indicates that Type II error was not a concern, confirming the adequacy of our sample size. Additionally, an important limitation of our study is that we were unable to follow the control group longitudinally over one year, as it was not possible to ensure that these participants would remain uninfected during the follow-up period. This limitation was largely due to the high rate of SARS-CoV-2 infection in the general population during the data collection period, which took place during the COVID-19 pandemic. As a result, many participants initially eligible for the control group were later excluded, compromising the feasibility of a consistent longitudinal assessment. Due to the observational design, factors such as new infections, physical activity levels, and potential treatments could not be controlled. Baseline clinical differences, especially in the severe COVID-19 group, who had higher BMI, more comorbidities, older age, and lower levels of physical activity, may be considered potential confounding factors. However, these characteristics are well-known risk factors strongly associated with progression to severe forms of COVID-19<sup>44</sup>. We believe that, rather than representing a methodological flaw, these findings reflect the true clinical profile of the most severely affected individuals, thereby enhancing the epidemiological and pathophysiological relevance of our results. Additionally, the choice of the GL muscle as a representative of the TS group is particularly appropriate for the assessment of NEDs. Although selected for technical feasibility, patient tolerability, and measurement reliability<sup>9</sup> it may not fully represent the physiological characteristics of the entire group, especially the SO muscle, which differs in fiber composition and function<sup>61</sup>. This choice was necessary due to the challenges of assessing the soleus muscle in this population, but it should be considered when interpreting the generalizability of the results. Finally, further studies are needed to assess long COVID patients beyond the one-year period.

### Conclusion

Individuals who had severe COVID-19 show a higher prevalence of NEDs in the TA muscle, associated with increased echogenicity that persists in all analyzed muscles, especially in the TA, over one year. Clinicians should consider the time elapsed since the COVID-19 diagnosis, the severity of the cases, and the assessed muscle when recommending more targeted treatment strategies for individuals with long COVID-19.

### Data availability

Data is provided within the manuscript or supplementary information files.

Received: 30 March 2025; Accepted: 21 August 2025

Published online: 02 October 2025

### References

1. Michaelson, N. M. et al. Peripheral neurological complications during COVID-19: A single center experience. *J. Neurol. Sci.* **434**, 120118 (2022).
2. Leonardi, M., Padovani, A. & McArthur, J. C. Neurological manifestations associated with COVID-19: a review and a call for action. *J. Neurol.* **267**, 1573–1576 (2020).

3. Abdullahi, A. et al. Neurological and musculoskeletal features of COVID-19: A systematic review and meta-analysis. *Front. Neurol.* **11**, 1–14 (2020).
4. Davis, H. E., McCorkell, L., Vogel, J. M. & Topol, E. J. Long COVID: major findings, mechanisms and recommendations. *Nat. Rev. Microbiol.* **21**, 133–146 (2023).
5. Aschman, T. et al. Association between SARS-CoV-2 infection and Immune-Mediated myopathy in patients who have died. *JAMA Neurol.* **78**, 948–960 (2021).
6. Ortelli, P. et al. Neuropsychological and neurophysiological correlates of fatigue in post-acute patients with neurological manifestations of COVID-19: insights into a challenging symptom. *J. Neurol. Sci.* **420**, 117271 (2021).
7. Taga, A. & Lauria, G. COVID-19 and the peripheral nervous system. A 2-year review from the pandemic to the vaccine era. *J. Peripheral Nerv. Syst.* **27**, 4–30 (2022).
8. Huang, L. et al. 1-year outcomes in hospital survivors with COVID-19: a longitudinal cohort study. *Lancet* **398**, 747–758 (2021).
9. da Silva Almeida, I. et al. Intra- and inter-rater reliability and agreement of stimulus electrodiagnostic tests in post-COVID-19 patients. *Physiol. Meas.* **44**, 055006 (2023).
10. Kubo, K. et al. Effects of 20 days of bed rest on the viscoelastic properties of tendon structures in lower limb muscles. *Br. J. Sports Med.* **38**, 324–330 (2004).
11. Silva, P. E. et al. Neuromuscular electrophysiological disorders and muscle atrophy in mechanically-ventilated traumatic brain injury patients: new insights from a prospective observational study. *J. Crit. Care.* **44**, 87–94 (2018).
12. Sullivan, B. N., Fischer, T. & Age-Associated Neurological Complications of COVID-19: A Systematic Review and Meta-Analysis. *Frontiers in Aging Neuroscience* vol. 13 Preprint at (2021). <https://doi.org/10.3389/fnagi.2021.653694>
13. Vieira, L. et al. Reliability of skeletal muscle ultrasound in critically ill trauma patients. *Rev. Bras. Ter. Intensiva.* **31**, 464–473 (2019).
14. Paternostro-Sluga, T., Schuhfried, O., Vacariu, G., Lang, T. & Fialka-Moser, V. Chronaxie and accommodation index in the diagnosis of muscle denervation. *Am. J. Phys. Med. Rehabil.* **81**, 253–260 (2002).
15. Schuhfried, O., Kollmann, C. & Paternostro-Sluga, T. Excitability of chronic hemiparetic muscles: determination of Chronaxie values and strength-duration curves and its implication in functional electrical stimulation. *IEEE Trans. Neural Syst. Rehabil. Eng.* **13**, 105–109 (2005).
16. Welch, C., Greig, C., Masud, T., Wilson, D. & Jackson, T. A. COVID-19 and acute sarcopenia. *Aging Dis.* **11**, 1345–1351 (2020).
17. Wall, B. T. et al. Substantial skeletal muscle loss occurs during only 5 days of disuse. *Acta Physiol.* **210**, 600–611 (2014).
18. Puthucherry, Z. A. et al. Qualitative ultrasound in acute critical illness muscle wasting. *Crit. Care Med.* **43**, 1603–1611 (2015).
19. de Andrade-Junior, M. C. et al. Skeletal muscle wasting and function impairment in intensive care patients with severe COVID-19. *Front. Physiol.* **12**, 1–13 (2021).
20. Appelman, B. et al. Muscle abnormalities worsen after post-exertional malaise in long COVID. *Nat. Commun.* **15**, 17 (2024).
21. de Ferreira, J. Intra- and Inter-Rater reliability and agreement of ultrasound imaging of muscle architecture and patellar tendon in Post-COVID-19 patients who had experienced moderate or severe COVID-19 infection. *J. Clin. Med.* **11**, 6934 (2022).
22. Santana, L. et al. Neuromuscular disorders in women and men with spinal cord injury are associated with changes in muscle and tendon architecture. *J. Spinal Cord Med.* **1–11** <https://doi.org/10.1080/10790268.2022.2035619> (2022).
23. Cuschieri, S. The STROBE guidelines. *Saudi J. Anaesth.* **13**, S31. [https://doi.org/10.4103/sja.SJA\\_543\\_18](https://doi.org/10.4103/sja.SJA_543_18) (2019). S34 Preprint at.
24. Siddiqi, H. K. & Mehra, M. R. COVID-19 illness in native and immunosuppressed states: A clinical–therapeutic staging proposal. *J. Heart Lung Transplantation.* **39**, 405–407 (2020).
25. Gandhi, R. T. & Lynch, J. B. Del rio, C. Mild or moderate Covid-19. *N. Engl. J. Med.* **383**, 1757–1766 (2020).
26. Krupp, L. B. & Pollina, D. A. Mechanisms and management of fatigue in progressive neurological disorders. *Curr. Opin. Neurol.* **9**, 456–460 (1996).
27. Botter, A. et al. Atlas of the muscle motor points for the lower limb: implications for electrical stimulation procedures and electrode positioning. *Eur. J. Appl. Physiol.* **111**, 2461–2471 (2011).
28. de Araujo, A. E. T. et al. Intra and inter-raters reliability and agreement of stimulus electrodiagnostic tests with two different electrodes in sedated critically-ill patients. *Physiother Theory Pract.* **36**, 1447–1456 (2020).
29. Fernandes, L. F. R. M. et al. Stimulus electrodiagnosis and motor and functional evaluations during ulnar nerve recovery. *Braz J. Phys. Ther.* **20**, 126–132 (2016).
30. Blazevich, A. J., Gill, N. D. & Zhou, S. Intra- and intermuscular variation in human quadriceps femoris architecture assessed in vivo. *J. Anat.* **209**, 289–310 (2006).
31. de Boer, M. D. et al. Effect of 5 weeks horizontal bed rest on human muscle thickness and architecture of weight bearing and non-weight bearing muscles. *Eur. J. Appl. Physiol.* **104**, 401–407 (2008).
32. Arts, I. M. P., Pillen, S., Schelhaas, H. J., Overeem, S. & Zwarts, M. J. Normal values for quantitative muscle ultrasonography in adults. *Muscle Nerve.* **41**, 32–41 (2010).
33. Geremia, J. M. et al. Triceps Surae muscle architecture adaptations to eccentric training. *Front. Physiol.* **10**, 1–10 (2019).
34. Kawakami, Y., Muraoka, T., Ito, S., Kanehisa, H. & Fukunaga, T. In vivo muscle fibre behaviour during counter-movement exercise in humans reveals a significant role for tendon elasticity. *J. Physiol.* **540**, 635–646 (2002).
35. Lima, K. M. M. & De Oliveira, L. F. Confiabilidade Das Medidas de arquitetura do músculo Vasto lateral Pela ultrassonografia. *Motriz Revista De Educacao Fisica.* **19**, 217–223 (2013).
36. Pillen, S. et al. Skeletal muscle ultrasonography: visual versus quantitative evaluation. *Ultrasound Med. Biol.* **32**, 1315–1321 (2006).
37. Pillen, S. et al. Skeletal muscle ultrasound: correlation between fibrous tissue and echo intensity. *Ultrasound Med. Biol.* **35**, 443–446 (2009).
38. Pan, W. Akaike's information criterion in generalized estimating equations. *Biometrics* **57**, 120–125 (2001).
39. Carolus, A. E. et al. The interdisciplinary management of foot drop. *Dtsch. Arztebl Int.* **116**, 347–354 (2019).
40. Stewart, J. D. Foot drop: Where, why and what to do? *Practical Neurology* vol. 8 158–169 Preprint at (2008). <https://doi.org/10.1136/jnnp.2008.149393>
41. Bowe, B., Xie, Y. & Al-Aly, Z. Postacute sequelae of COVID-19 at 2 years. *Nat. Med.* **29**, 2347–2357 (2023).
42. Huang, C. et al. 6-month consequences of COVID-19 in patients discharged from hospital: a cohort study. *Lancet* **401**, e21–e33 (2023).
43. Garibaldi, B. T. et al. Patient trajectories among persons hospitalized for COVID-19. *Ann. Intern. Med.* **174**, 33–41 (2021).
44. Guan, W. et al. Comorbidity and its impact on 1590 patients with COVID-19 in china: a nationwide analysis. *Eur. Respir. J.* **55**, 2000547 (2020).
45. Zhang, J., jin, Dong, X., Liu, G. & Gao, Y. Risk and Protective Factors for COVID-19 Morbidity, Severity, and Mortality. *Clinical Reviews in Allergy and Immunology* vol. 64 90–107 Preprint at (2023). <https://doi.org/10.1007/s12016-022-08921-5>
46. Mao, L. et al. Neurologic manifestations of hospitalized patients with coronavirus disease 2019 in wuhan, China. *JAMA Neurol.* **77**, 683–690 (2020).
47. Parry, S. et al. (ed, M.) Ultrasonography in the intensive care setting can be used to detect changes in the quality and quantity of muscle and is related to muscle strength and function. *J. Crit. Care* **30** 1151e9–1151e14 (2015).
48. Andalib, S. et al. Peripheral nervous system manifestations associated with COVID-19. *Curr. Neurol. Neurosci. Rep.* **21**, 9 (2021).
49. Silva-Hernández, L., Cabal-Paz, B., Mayo-Canalejo, D. & Horga, A. Post-COVID symptoms of potential peripheral nervous and muscular origin. *Neurol. Perspect.* **1** <https://doi.org/10.1016/j.neurop.2021.11.002> (2021). S25–S30 Preprint at.
50. Silva, P. E. et al. Safety and feasibility of a neuromuscular electrical stimulation chronaxie-based protocol in critical ill patients: A prospective observational study. *J. Crit. Care.* **37**, 141–148 (2017).

51. Terlemez, R., Misirlioglu, T. Ö., Palamar, D., Okutan, D. & Akgün, K. Bilateral foot drop after COVID-19-related acute respiratory distress syndrome: A case report. *Turk. J. Phys. Med. Rehabil.* **67**, 378–381 (2021).
52. Andiappan, K., Nyein Yin, K. & Zainudin, M. F. Unilateral compressive peroneal neuropathy in intensive care settings during the COVID-19 pandemic: A series of three cases. *Cureus* <https://doi.org/10.7759/cureus.65789> (2024).
53. Chang, L. G., Zar, S., Seidel, B., Kurra, A. & Gitkind, A. COVID-19 prone ventilation and its possible association with foot drop: A case series. *Cureus* **13**, 8–11 (2021).
54. Taketa, T., Uchiyama, Y., Kodama, N., Koyama, T. & Domen, K. ICU-Acquired weakness complicated with bilateral foot drop after severe COVID-19: successful rehabilitation approach and Long-Term Follow-Up. *Cureus* <https://doi.org/10.7759/cureus.36566> (2023).
55. Zavaroni, S. et al. Ultrasound-based neuropathy diagnosis in COVID-19 patients in Post-intensive care rehabilitation settings: A retrospective observational study. *Arch. Phys. Med. Rehabil.* **104**, 1236–1242 (2023).
56. Soares, M. N. et al. Skeletal muscle alterations in patients with acute Covid-19 and post-acute sequelae of Covid-19. *J. Cachexia Sarcopenia Muscle.* **13**, 11–22 (2022).
57. Narici, M., Franchi, M. & Maganaris, C. Muscle structural assembly and functional consequences. *Journal of Experimental Biology* vol. 219 276–284 Preprint at (2016). <https://doi.org/10.1242/jeb.128017>
58. Grimm, A. et al. Muscle ultrasound for early assessment of critical illness neuromyopathy in severe sepsis. *Crit. Care* **17**, 1–11 (2013).
59. Kerbaul, F. et al. Combination of histopathological and electromyographic patterns can help to evaluate functional outcome of critical ill patients with neuromuscular weakness syndromes. *Crit. Care.* **8**, R358 (2004).
60. Dalmau-Pastor, M., Fargues-Polo, B., Casanova-Martínez, D., Vega, J. & Golanó, P. Anatomy of the triceps surae: A pictorial essay. *Foot Ankle Clin.* **19**, 603–635 (2014).

## Acknowledgements

The authors would like to thank all the individuals who participated in this study.

## Author contributions

RCM and JLQD conceived the idea for and designed the study. They had full access to all the data in the study and took responsibility for the integrity of the data and the accuracy of the data analysis. ISA, JLQD, RCM, LGJF, MAV, RRC, NB, and GCJ drafted the paper. ISA, LGJF and RRC conducted the analysis, and all authors critically revised the manuscript for significant intellectual content and agreed to submit the final version for publication. ISA and LGJF completed the follow-up work. ISA, LGJF and JLQD collected and verified the data. All authors agree to be accountable for all aspects of the work, ensuring that questions related to the accuracy or integrity of any part of the work are appropriately investigated and resolved.

## Funding

This work was supported by the Coordenação de Aperfeiçoamento de Pessoal de Nível Superior – Brasil (CAPES) [Finance Code 001]; Fundação de Apoio à Pesquisa do Distrito Federal (FAPDF) [Grant Numbers 00193.00000669/2025-10; 00193.00000773/2021-72, 00193.00000859/2021-3; 00193.00001222/2021-26, 00193-00001261/2021-23; 000193-00002357 and 00193-00001132/2024-88], and Conselho Nacional de Desenvolvimento Científico e Tecnológico (CNPq) [Grant numbers 309435/2020-0, 310269/2021-0, 141130/2023-7, 308519/2025-6 and 131422/2023-5].

## Declarations

### Competing interests

The authors declare no competing interests.

### Additional information

**Supplementary Information** The online version contains supplementary material available at <https://doi.org/10.1038/s41598-025-17126-7>.

**Correspondence** and requests for materials should be addressed to I.S.A. or J.L.Q.D.

**Reprints and permissions information** is available at [www.nature.com/reprints](http://www.nature.com/reprints).

**Publisher's note** Springer Nature remains neutral with regard to jurisdictional claims in published maps and institutional affiliations.

**Open Access** This article is licensed under a Creative Commons Attribution-NonCommercial-NoDerivatives 4.0 International License, which permits any non-commercial use, sharing, distribution and reproduction in any medium or format, as long as you give appropriate credit to the original author(s) and the source, provide a link to the Creative Commons licence, and indicate if you modified the licensed material. You do not have permission under this licence to share adapted material derived from this article or parts of it. The images or other third party material in this article are included in the article's Creative Commons licence, unless indicated otherwise in a credit line to the material. If material is not included in the article's Creative Commons licence and your intended use is not permitted by statutory regulation or exceeds the permitted use, you will need to obtain permission directly from the copyright holder. To view a copy of this licence, visit <http://creativecommons.org/licenses/by-nc-nd/4.0/>.

© The Author(s) 2025